Published in *Manufacturing Letters*, Volume 24, April 2020, Pages 82-86

Synthesis and machining characteristics of novel TiC ceramic and MoS_2 soft particulate reinforced aluminium alloy 7075 matrix composites

Anvesh Dhulipalla[1], Budireddy Uday Kumar [2], Varupula Akhil[2], Jian Zhang[1], Zhe Lu[3], Hye-Yeong Park[4], Yeon-Gil Jung[4], Jing Zhang [1*]

[1]Department of Mechanical and Energy Engineering, Indiana University – Purdue University Indianapolis, Indiana 46202, USA

[2]School of Mechanical Engineering, Vellore Institute of Engineering, Vellore 632014, Tamil Nadu, India

3. School of Materials and Metallurgical Engineering, University of Science and Technology of Liaoning, China

4. Changwon National University, Changwon, Gyeongnam, Republic of Korea

*Corresponding author: jz29@iupui.edu; Tel: +1-3172787186; Fax: +1-3172749744

Abstract

In this work, the synthesis and machinability studies are presented for a new TiC ceramic and MoS_2 soft particulate reinforced aluminium alloy 7075 (AA7075) matrix composite (AMCs). The results show that the AMCs have improved machinability compared with the base AA7075. The chip morphology is changed from continuous sheared chips in AA7075 to discontinuous chips in AMCs. The change is caused by the reduced ductility in AMCs due to

reinforcement TiC and MoS_2 microparticles. The surface roughness is increased for the AMCs when compared to that of base alloy due to hard TiC particles.

Keywords: Aluminium matrix composite; Tool wear; Chip formation; Surface roughness

1. Introduction

A metal matrix composite (MMC) is a composite material with two constituent parts, one is a metal necessarily, other may be a metal or ceramic or an organic compound. The matrix is a single continuous phase into which reinforcements are added. Unlike two materials are sandwiched together, there is a path through the matrix to any point in the material. The reinforcements are not only used for structural propose, but also can be used to change the physical properties such as thermal conductivity, and wear resistance [1-5].

There are different methods for manufacturing MMCs: solid, liquid, and vapour states. Liquid method of processing is preferred because of its ease of adoption, simplicity and applicability to mass production. In the liquid method, the aluminium matrix is completely melted and ceramic particles are added into the molten metal. Aluminium alloys are one of the most commonly used metallic materials as a matrix in MMCs because of its high strength to weight ratio and low costs.

Aluminium alloys can be reinforced with ceramic particles [6, 7], such as B_4C, TiB_2, Al_2O_3, SiC, and TiC to form aluminium metal matrix composites (AMCs). In this work presented here, the two reinforcements used are titanium carbide (TiC) and molybdenum disulfide(MoS_2). Titanium carbide is an extremely hard refractory ceramics with a high melting temperature of 3160 °C. Molybdenum disulfide, MoS_2, is a soft material and used as dry lubricant due to its low coefficient of friction [8].

There are several previous studies on machining of aluminium and its alloy. Garg *et al.* provided a review on the recent research progresses in aluminium matrix composites [9]. The commonly used synthesis routes, mechanical behavior and applications of aluminium matrix composites are summarized in Ref. [9]. Hamouda and Hashmi developed a flow stress model based on plasticity for aluminium metal matrix composite materials subjected to high strain rate [10]. The parameters of the proposed flow stress model were evaluated based on good

agreement between the predicted and measured final dimension of the test specimen [10]. Pattnaik *et al.* studied that formation of a built-up edge (BUE) which can be reduced by choosing appropriate combination of cutting speed, feed, and cutting tool material[11]. Carrilero *et al.* showed that dry machining is preferred due to the fact that there is no need of cutting fluid and associate environmental concerns [12]. In Ref. [13], the effects of SiC-particulate reinforcement to AA7075 on surface roughness and tool wear during turning have been investigated in terms of selected parameters such as cutting speeds, feed rates, and depth of cuts [10]. Based on the results of surface roughness in the work piece and flank wear in the tool, it is recommended that turning operation on Al alloy composite by polycrystalline diamond insert should be carried out at cutting speed higher than 220 m/min but at a feed rate of less than 0.2 mm/rev and depth of cut less than 1.0 mm [13]. Guan *et al.* developed aluminium matrix composites reinforced with metallic glass particles with core-shell structure by combining spark plasma sintering with hot rolling [14]. The results showed that the shell zone is helpful to improve the mechanical properties of the composites [14]. Abraham *et al.* studied vanadium particles reinforced AA6063 aluminium matrix composites via friction stir processing[15]. The vanadium particles improved tensile strength without major loss in ductility [15].

Although these previous efforts, there is still a need to improve the machinability of aluminium alloys for fully explore their potentials. In this work, we develop a new type of AA7075/TiC/MoS_2 AMC and investigate its machining characteristics. The new developed AMC is expected to have improved machinability for many industrial applications. The structure of the paper is arranged as follows. In Section 2, the experimental synthesis procedure of the AMCs using stir casting technique is described. The procedures of machining characteristics study and microstructure analysis are provided. In Section 3, the results and discussion of the studies are presented, which include the density and hardness measurements

of the synthesized AMCs, microscopic analysis, and flank wear. In Section 4, the conclusions are summarized.

2. Experimental procedure

2.1 Synthesis of AMCs

In this work, stir casting technique was used to synthesize the AMCs. Stir casting is selected because it is one of the methods accepted for the production of large quantity commercially practised. It is attractive due to its simplicity, flexibility and most economical for large sized components to be fabricated [16, 17].

To achieve the designed AMC compositions, for each sample, 800 g of aluminium and respective wt.% of TiC (2% and 4%), MoS_2(0% and 2%) reinforcements were taken and weighed accordingly. The compositions of samples are base material (AA7075), AA7075 + TiC (2%), AA7075 + TiC (4%), AA7075 + TiC (2%) + MoS_2 (2%), and AA7075 + TiC (4%) + MoS_2 (2%). The base material AA7075 was taken as small ingots of 60 mm in length and diameter of approximately 30 mm, and its nominal chemical composition is (wt.%), 0.10 Si, 0.23 Fe, 1.48 Cu, 0.07 Mn, 2.11 Mg, 0.22 Cr, 0.01 Ni, 5.29 Zn, 0.07 Ti, 0.02Zr, and balance Al.

The stir casting process of the AMCs is illustrated in Fig. 1. As shown in the figure, reinforcements and the die are preheated using a die heating furnace at 250 ºC, and later the furnace of the stir casting facility reaches 750 ºC. Once it achieves the required temperature, aluminium pieces are kept in the furnace and are left to melt. Once the furnace reaches 850 ºC, another 30 more minutes are required until it is completely melted. Then the reinforcements are added into the furnace through a small orifice of a cone shaped dipper. Then the stirrer is inserted mechanically and the motor is switched on and kept at 700 rpm. The stirrer is pulled

out after 10 minutes and then the slag is removed. After the slag is removed, the stirrer is inserted again into the furnace. The die is kept directly below the pouring slot. After 5 minutes of stirring, the stirrer is removed from the furnace and the motor is switched off. Then the down pouring process starts. The whole molten mixture is poured into the die. Any remains should be removed from the furnace. The die is then cooled and the cylindrical sample is removed carefully. The die is again reassembled and placed in the die heater for the next operation. The specimens are polished and etched using 1% HF solution and observed using a metallurgical microscope.

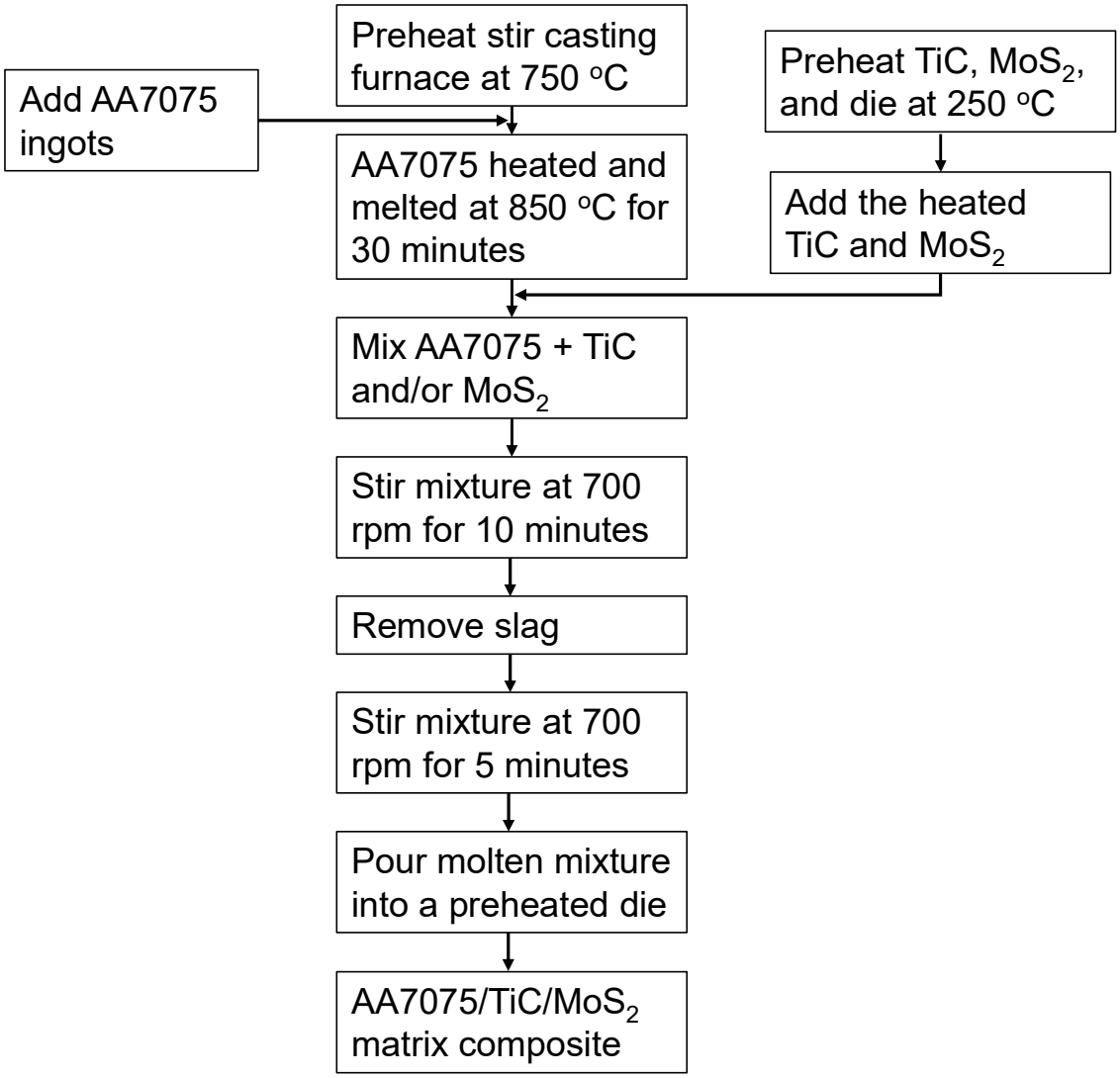

Figure 1: Flow chart of stir casting process of AA7075/TiC/MoS_2 matrix composites.

2.2 Machining characteristics study

Turning experiments conditions were carried out in a computer numerical lathe (CNC) lathe (CNMG 120408 ML WP28CT, TaeguTec Ltd. Republic of Korea), which is a TiN coated carbide cutting tool. The turning conditions are as follows: nose radius 0.8 mm; cutting speeds 30, 60 and 90 m/min; feed rate 0.05 mm/rev; depths of cut 0.5,1.0 and 1.5 mm; and the cutting condition is dry. Three samples are selected for machinability study: AA7075; Al + TiC (2%)

+ MoS_2 (2%); and Al + TiC (4%) + MoS_2 (2%). Additionally, the hardness of all the samples were measured using a Rockwell hardness tester (Model No. 900-331, Metal-Testers).

2.3 Microstructure analysis

After the turning experiments, the chips were carefully collected. The microstructures were examined using a Field Emission-Scanning Electron Microscope (FE-SEM, FEI Quanta 250 FEG). The surface roughness of the machined samples was found by using a surface roughness tester (Pocketsurf IV, Mahr GmbH, Germany). The tool wear and chips were observed by using a digital microscope (Dino-Lite Edge 3.0, AnMo Electronics Corporation, China).

3. Results and discussion

3.1 Hardness and density

The measured Rockwell Hardness (HRB) values are 52.5±1.5 (AA7075), 67.2±2.2 (Al+TiC (2%)), 75.4±4.3 (Al+TiC (4%)), 54.1±2.4 (Al+TiC (2%)+MoS_2(2%)), and 61.9±6.6 (Al+TiC (4%)+MoS_2(2%)). The hardness data show that the hardness of all the castings had been increased considerably compared to base alloy. Comparing AA7075, Al+TiC (2%), and Al+TiC (4%), the hardness increased with increasing amount of TiC, since TiC is a hard ceramic material. With the addition of MoS_2 in the above AMCs, the hardness values had been reduced, which is due to the soft phase MoS_2. Additionally, the measured densities of TiC ceramic and MoS_2 nanoparticles are found to be more than that of base alloy and contributed to marginal increase as compared to AA7075.

3.2 Microstructures of AMCs

Fig. 2 shows all the microstructures of the wrought AA7075 and AMCs. In Fig. 2a, the wrought AA7075, it shows coarse elongated Al grains and $Mg(Al,Cu,Zn)_2$ intermetallic compounds that precipitated along the Al grain boundaries [18]. There is a significant number

of intermetallic compounds and eutectic phases $Mg(Al,Cu,Zn)_2$ composed of Zn, Mg, Cu. Al usually distribute along the grain boundaries [18]. The eutectic phases have been reported previously which are related to a reduction in mechanical properties after heat treatment and hot deformation processes [19, 20].

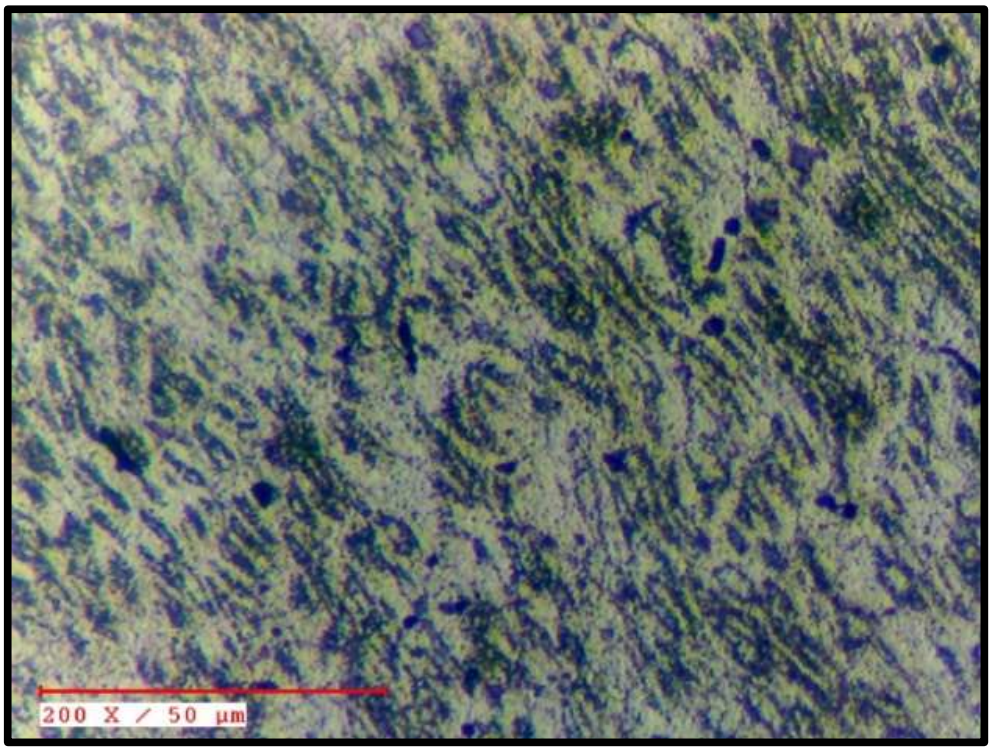

(a)

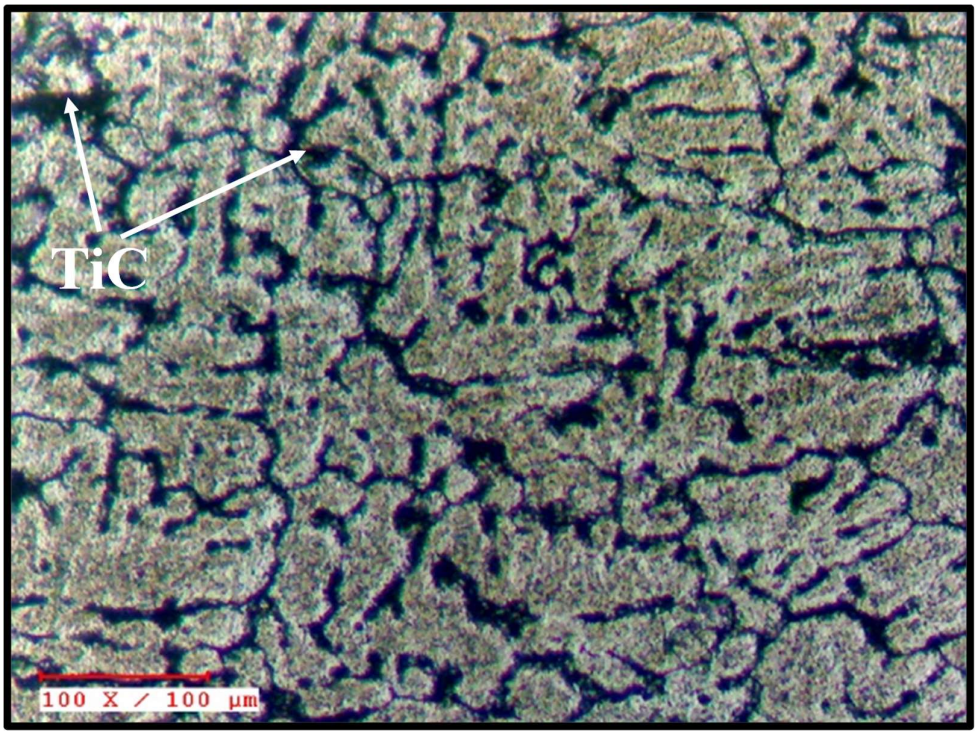

(b)

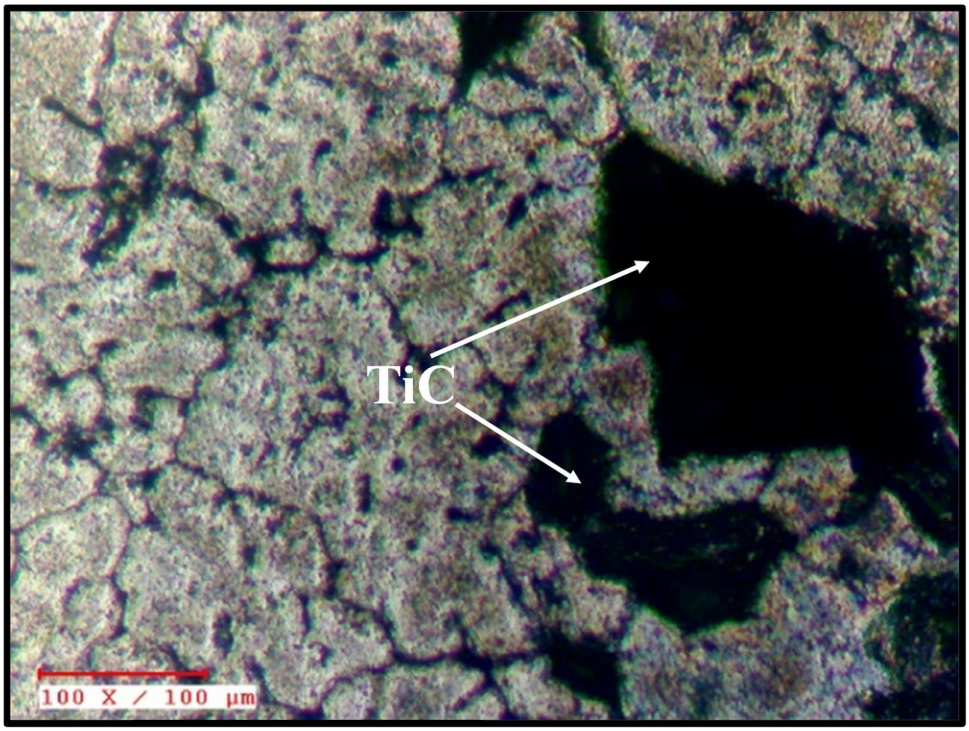

(c)

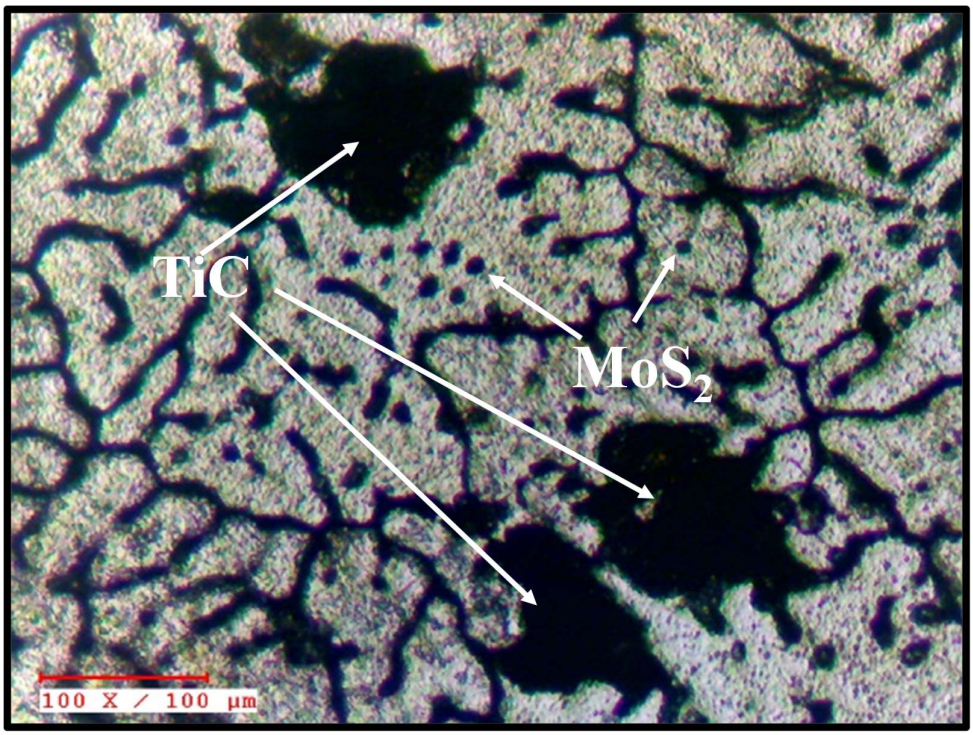

(d)

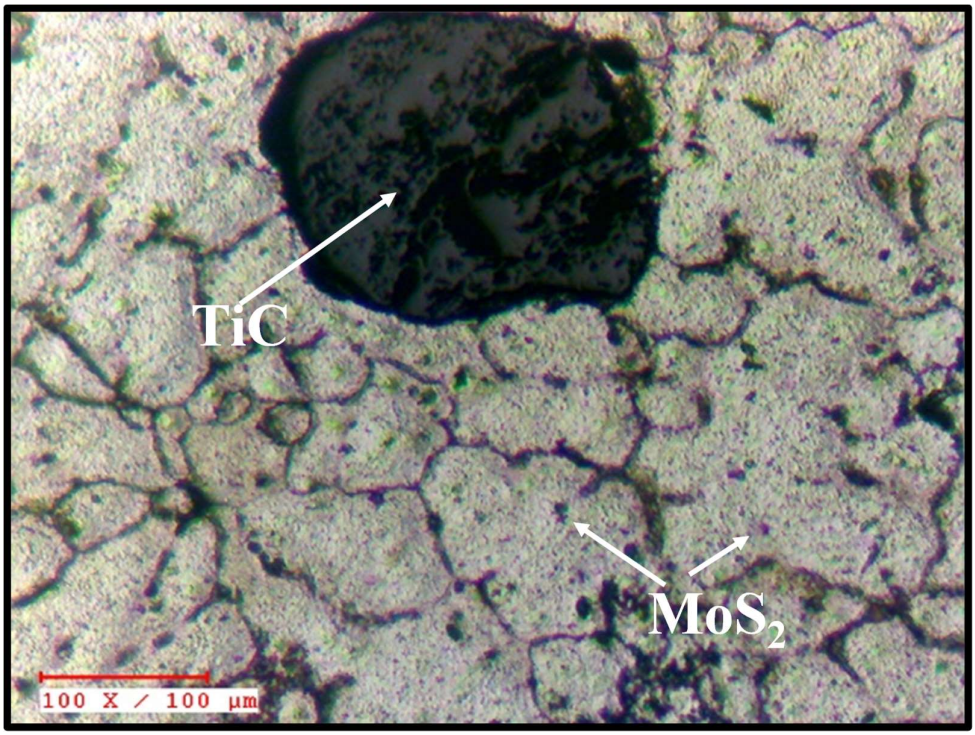

(e)

Figure 2: Microstructures of (a) wrought AA7075, where the white region is Al, and the dark region is the eutectic phase $Mg(Al,Cu,Zn)_2$. (b) AA7075 + (2%) TiC, where the black region is TiC as marked, and the white region is Al. (c) AA7075 + (4%) TiC, where the black region is TiC as marked, and the white region is Al. (d) AA7075 + (2%) TiC + (2%) MoS_2. (e) AA7075 + (4%) TiC + (2%) MoS_2.

The microstructure of the cast AA7075 + (2%) TiC is shown in Fig. 2b. There are randomly scattered titanium carbide (TiC) particles in the AA7075 matrix. The TiC particles have an average particle size of 20 μm. Also as shown in the figures, all the Al grains are surrounded by TiC. This is because TiC particles serve as the nucleation sites for Al grains due to their small lattice mismatch between Al and TiC [21].

The microstructure of the cast AA7075 + (4%) TiC is shown in Fig. 2c. Compared with the low concentration of 2% TiC shown in Fig. 2b, the 4% TiC case in Fig.2c has much larger TiC particles with an average particle size of 50 μm, likely due to glomeration during the mixing process. Moreover, Fig. 2c also shows that the Al grains have a dendritic structure, similar to the AA7075 + (2%) TiC in Fig. 2b. However the aspect ratio of the Al grains is smaller than the one in in Fig. 2b, suggesting increased TiC particles serve as the barrier of the Al grains, hindering their dendrite growth during the solidification process.

The microstructure AA7075 + (2%) TiC + (2%) MoS_2 is shown in Fig. 2d. Within the AA7075 matrix, there are randomly scattered large TiC particles and MoS_2 microparticles. The MoS_2 nanoparticles are embedded in the Al grains and $Mg(Al,Cu,Zn)_2$ intermetallic compounds. There is no chemical reaction between the reinforcements and matrix.

Fig. 2e shows the microstructure of AA7075 + (4%) TiC + (2%) MoS_2. The TiC particle is much greater than the case in Fig.2d due to higher concentration of TiC. Similar to Fig. 2d, the MoS_2 microparticles are embedded in the Al grains and $Mg(Al,Cu,Zn)_2$ intermetallic compounds.

3.3 Flank wear

The effect of cutting speed (30, 60, and 90 m/min) and cutting depth (0.5, 1.0, and 1.5 mm) on flank wear is studied. The flank wear amounts increase dramatically for both AA7075 (80 ~ 140 μm) and AMCs (130 ~ 170 μm) with increasing cutting depth. In comparison, the flank wear is only moderately changed about 10 μm within the tested cutting speeds.

The side views of the tool rake are given in Fig. 3. The built-up edge (BUE) is formed in most cases. In a few cases, there was a nose worn out. In the case of AA7075 shown in Fig. 3a, crater wear on the cutting edge was observed with the BUE of ~ 150 μm. In comparison, for the AMC shown in Fig. 3b, the thickness of BUE is only 90 μm, suggesting a stable state in the AMC machining process, which also helps reduce the tooling wear.

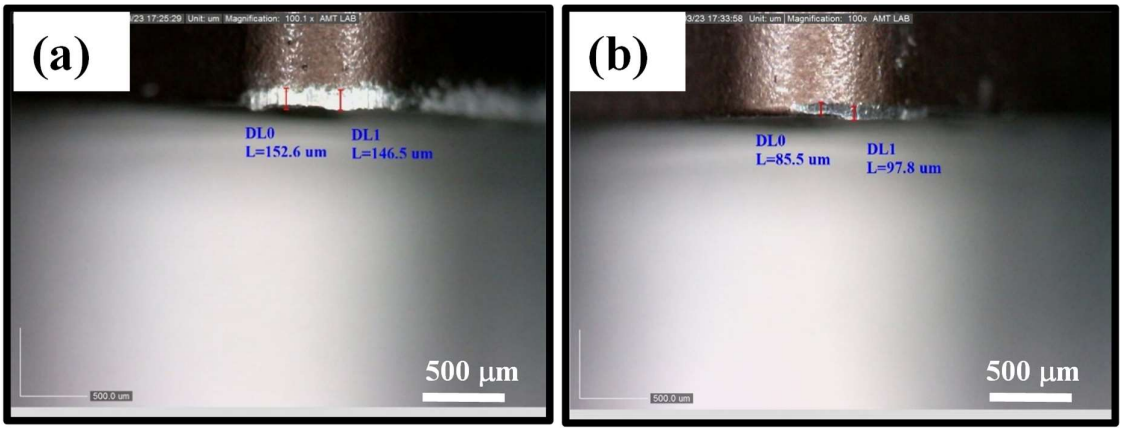

Figure 3: Side views of after machining tool surface. (a) Worn out case at the nose in AA7075, (b) Little wear out case in AMCs.

3.4 Surface roughness

The effect of cutting speed (30, 60, and 90 m/min) and cutting depth (0.5, 1.0, and 1.5 mm) on the surface roughness is studied and measured using a surface roughness tester. The surface roughness increases with the increasing cutting depth and cutting speed. At the cutting speed and cutting depth ranges specified above, the surface roughness increased from 0.15 ~ 0.35 μm for AA7075; 0.38 ~ 0.46 μm for AA7075 + TiC (2%) + MoS_2 (2%); and 0.54 ~ 0.62 AA7075 + TiC (4%) + MoS_2 (2%). The increased surface roughness in the AMCs is due to the added TiC particles.

As the base alloy AA7075 is softer than the cast AMCs, its surface is found to be less rough. In case of AMCs, as the amount of TiC is increasing, the surface roughness is also increasing due to the hard TiC particles. However, the formed porosity may be an issue, because of which poor surface finish was observed.

3.5 Chip morphology

The examples of photograph of the formed chips formed in AA7075, Al + TiC (2%) + MoS_2 (2%), and Al + TiC (4%) + MoS_2 (2%) AMCs are shown in Fig. 4. For AA7075 shown in Fig. 4a, the chips are continuous and showed spiral and curling morphology. This type of chips is called Sheared Chips or Continuous Chip with a Built-up Edge (BUE), commonly seen in ductile metals [22]. The metal ahead of the cutting tool is compressed and forms a chip which begins to flow along the chip-tool interface. As a result of the high temperature, the high pressure, and the high frictional resistance against the flow of the chip along the chip-tool interface, small particles of metal begin adhering to the edge of the cutting tool while the chip shears away [22].

From samples of (2% and 4%)TiC/ (2%)MoS_2 AMCs in Figs. 4b and 4c, the chips produced are in discontinuous form. Discontinuous or segmented chips are produced when brittle metals are cut or when some ductile metals are cut under poor cutting conditions [22]. As the point of the cutting tool contacts the metal, some compression occurs, and the chip begins flowing along the chip-tool interface. As more stress is applied to brittle metal by the cutting action, the metal compresses until it reaches a point where rupture occurs and the chip separates from the unmachined portion [22]. Therefore, AMCs improve the Al7075's machinability through changing the continuous sheared chips to discontinuous chips.

However, close observations also show that there are deep cracks on the chip propagating from the free end in the AMC samples. Crack propagation is visible clearly in the samples. This shows that addition of TiC and MoS_2 reinforcements reduces the ductility of the AMCs. The discontinuous chips cause fracture on the sample surfaces. Hence, increase in the content of TiC increases the surface roughness, as discussed in Section 3.4.

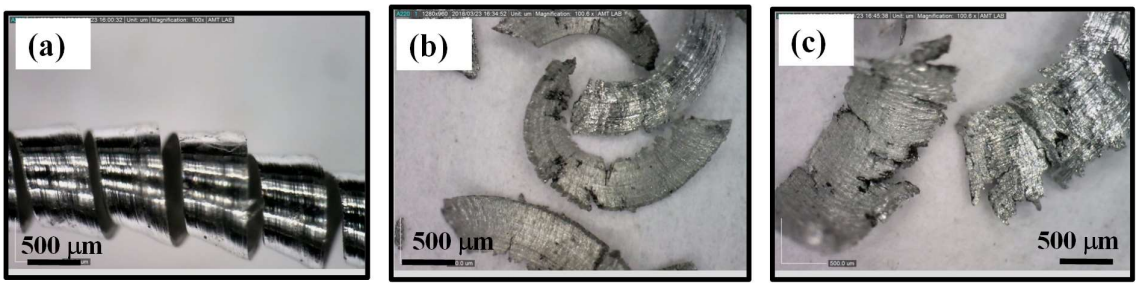

Figure 4: Photo graphs of the formed chips. (a) AA7075, (b) Al + TiC (2%) + MoS_2 (2%), (c) Al + TiC (4%) + MoS_2 (2%). The scale

4. Conclusions

In this work, new AA7075/ (0%, 2% and 4%)TiC/ (0% and 2%)MoS_2 AMCs were successfully synthesized, and the their machinability was studied. The major conclusions are summarized as follows.

1. Using stir casting process, the synthesized AMCs microstructures show that the TiC and MoS_2 microparticles are randomly scattered in the AA7075 matrix.
2. The AMCs have improved machinability compared with the base AA7075. The chip morphology is changed from continuous sheared chips in AA7075 to discontinuous chips in AMCs. The change is caused by the reduced ductility in AMCs due to reinforcement TiC and MoS_2 microparticles.
3. The surface roughness of AMCs is higher than that of the base AA7075, which is caused by the hard TiC content.

Acknowledgements

This work is partially supported by "Human Resources Program in Energy Technology (No. 20194030202450)" of the Korea Institute of Energy Technology Evaluation and Planning (KETEP). ZL acknowledges the financial support provided by the National Natural Science Foundation of China (No. 51702145), and innovation group project from the University of Science and Technology Liaoning (2017TD01).

References

[1] X.-s. Jiang, N.-j. Wang, and D.-g. Zhu, "Friction and wear properties of in-situ synthesized Al2O3 reinforced aluminum composites," *Transactions of Nonferrous Metals Society of China,* vol. 24, pp. 2352-2358, 2014/07/01/ 2014.

[2] B. Ashok Kumar and N. Murugan, "Metallurgical and mechanical characterization of stir cast AA6061-T6–AlNp composite," *Materials & Design,* vol. 40, pp. 52-58, 2012/09/01/ 2012.

[3] K. J. Lijay, J. D. R. Selvam, I. Dinaharan, and S. J. Vijay, "Microstructure and mechanical properties characterization of AA6061/TiC aluminum matrix composites synthesized by in situ reaction of silicon carbide and potassium fluotitanate," *Transactions of Nonferrous Metals Society of China,* vol. 26, pp. 1791-1800, 2016/07/01/ 2016.

[4] X.-f. Tan, F.-h. Zeng, S.-q. Wang, F. Zhou, and X. Xiong, "Effects of heat treatment on phase contents and mechanical properties of infiltrated B4C/2024Al composites," *Transactions of Nonferrous Metals Society of China,* vol. 24, pp. 2359-2365, 2014/07/01/ 2014.

[5] K. K. Chawla, "Metal Matrix Composites," in *Materials Science and Technology*, ed.

[6] Y.-C. Kang and S. L.-I. Chan, "Tensile properties of nanometric Al2O3 particulate-reinforced aluminum matrix composites," *Materials Chemistry and Physics,* vol. 85, pp. 438-443, 2004/06/15/ 2004.

[7] A. Sabahi Namini, M. Azadbeh, and M. Shahedi Asl, "Effect of TiB2 content on the characteristics of spark plasma sintered Ti–TiBw composites," *Advanced Powder Technology,* vol. 28, pp. 1564-1572, 2017/06/01/ 2017.

[8] R. Bissessur and P. K. Y. Liu, "Direct insertion of polypyrrole into molybdenum disulfide," *Solid State Ionics,* vol. 177, pp. 191-196, 2006/01/16/ 2006.

[9] P. Garg, A. Jamwal, D. Kumar, K. K. Sadasivuni, C. M. Hussain, and P. Gupta, "Advance research progresses in aluminium matrix composites: manufacturing & applications," *Journal of Materials Research and Technology,* vol. 8, pp. 4924-4939, 2019/09/01/ 2019.

[10] A. M. S. Hamouda and M. S. J. Hashmi, "Mechanical properties of aluminium metal matrix composites under impact loading," *Journal of Materials Processing Technology,* vol. 56, pp. 743-756, 1996/01/01/ 1996.

[11] S. Kanta Pattnaik, N. Bhoi, S. Padhi, and S. Kumar Sarangi, "Dry machining of aluminum for proper selection of cutting tool: tool performance and tool wear," *The International Journal of Advanced Manufacturing Technology,* vol. 98, pp. 1-11, 09/01 2018.

[12] M. S. Carrilero, R. Bienvenido, J. M. Sánchez, M. Álvarez, A. González, and M. Marcos, "A SEM and EDS insight into the BUL and BUE differences in the turning processes of AA2024 Al-Cu alloy," *International Journal of Machine Tools and Manufacture,* vol. 42, pp. 215- 220, 2002.

[13] R. K. Bhushan, S. Kumar, and S. Das, "Effect of machining parameters on surface roughness and tool wear for 7075 Al alloy SiC composite," *The International Journal of Advanced Manufacturing Technology,* vol. 50, pp. 459-469, September 01 2010.

[14] H. D. Guan, C. J. Li, P. Gao, K. G. Prashanth, J. Tan, J. Eckert*, et al.*, "Aluminum matrix composites reinforced with metallic glass particles with core-shell structure," *Materials Science and Engineering: A,* vol. 771, p. 138630, 2020/01/13/ 2020.

[15] S. J. Abraham, I. Dinaharan, J. D. Raja Selvam, and E. T. Akinlabi, "Microstructural characterization of vanadium particles reinforced AA6063 aluminum matrix composites via friction stir processing with improved tensile strength and appreciable ductility," *Composites Communications,* vol. 12, pp. 54-58, 2019/04/01/ 2019.

[16] J. Hashim, L. Looney, and M. S. J. Hashmi, "Metal matrix composites: production by the stir casting method," *Journal of Materials Processing Technology,* vol. 92-93, pp. 1-7, 1999/08/30/ 1999.

[17] S. B. Prabu, L. Karunamoorthy, S. Kathiresan, and B. Mohan, "Influence of stirring speed and stirring time on distribution of particles in cast metal matrix composite," *Journal of Materials Processing Technology,* vol. 171, pp. 268-273, 2006/01/20/ 2006.

[18] M. Zuo, M. Sokoluk, C. Cao, J. Yuan, S. Zheng, and X. Li, "Microstructure Control and Performance Evolution of Aluminum Alloy 7075 by Nano-Treating," *Scientific Reports,* vol. 9, p. 10671, 2019/07/23 2019.

[19] S. H. Seyed Ebrahimi and M. Emamy, "Effects of Al–5Ti–1B and Al–5Zr master alloys on the structure, hardness and tensile properties of a highly alloyed aluminum alloy," *Materials & Design,* vol. 31, pp. 200-209, 2010/01/01/ 2010.

[20] J. Dong, J. Z. Cui, F. X. Yu, Z. H. Zhao, and Y. B. Zhuo, "A new way to cast high-alloyed Al–Zn–Mg–Cu–Zr for super-high strength and toughness," *Journal of Materials Processing Technology,* vol. 171, pp. 399-404, 2006/02/01/ 2006.

[21] A. K. P. Rao, K. Das, B. S. Murty, and M. Chakraborty, "Al–Ti–C–Sr master alloy—A melt inoculant for simultaneous grain refinement and modification of hypoeutectic Al–Si alloys," *Journal of Alloys and Compounds,* vol. 480, pp. L49-L51, 2009/07/08/ 2009.

[22] *Chip Formation (https://www.destinytool.com/chip-formation.html, accessed 1/20/2020)*.